Dynamic Coarsening for Efficient Simulation of Geothermal Energy Applications

Øystein S. Klemetsdal

Department of Mathematics and Cybernetics, SINTEF Digital, Norway

InterPore 2021
Online, 1–4 June 2021

Introduction

- Hot underground aquifers are appealing resources for energy production and storage
  - Renewable ✓ Always on ✓ Available anywhere ✓
- Viability depends a number of factors (Glassley [2010], Stober and Bucher [2013])
  - Efficiency, storage capacity, operational and drilling costs, legal regulations, ...
- Assessment requires solid system knowledge (Andersson [2007])
  - Aquifer/aquiclude geology, groundwater chemistry, flow properties, ...

Introduction

- Hot underground aquifers are appealing resources for energy production and storage
  - Renewable ✓ Always on ✓ Available anywhere ✓
- Viability depends a number of factors (Glassley [2010], Stober and Bucher [2013])
  - Efficiency, storage capacity, operational and drilling costs, legal regulations, ...
- Assessment requires solid system knowledge (Andersson [2007])
  - Aquifer/aquiclude geology, groundwater chemistry, flow properties, ...

0.953.5em Complexity and size typically renders numerical simulations the only viable option (O'Sullivan et al. [2000], Lee [2010], Stober and Bucher [2013])

Introduction

Motivation

- Transport of geothermal heat chiefly confined to proximity of wells
- Difficult to determine appropriate grid resolution apriori
- Many geomodels not suitable for conventional grid refinement methods

Motivation

- Transport of geothermal heat chiefly confined to proximity of wells
- Difficult to determine appropriate grid resolution apriori
- Many geomodels not suitable for conventional grid refinement methods
- Reservoir engineering applications:

$$\#\ \text{cells in simulation grid} \quad \ll \quad \#\ \text{cells in geocellular model}$$

- State-of-the-art multiscale methods (attempt to) bridge gap for pressure problems [Jenny et al., 2006, Møyner and Lie, 2016, Lie et al., 2017], etc.
- Here: attempt to bridge this gap for transport problems by **dynamic coarsening**
  - Implementation in the MATLAB Reservoir Simulation Toolbox (MRST)

Governing equations and discretization

- Single-phase conservation of mass on semi-discrete, implicit form

$$R_f^{n+1} = \frac{1}{\Delta t^n}(M_f^{n+1} - M_f^n) + \nabla \cdot \vec{V}_f^{n+1} - Q_f = 0$$

Mass — Flux — Sources/sinks

  - Mass flux from Darcy's law: $\vec{V}_f = -\frac{\rho_f}{\mu_f}\mathrm{K}(\nabla p - \rho_f \vec{g})$

Governing equations and discretization

- Conservation of energy on semi-discrete, implicit form

$$R_e^{n+1} = \frac{1}{\Delta t^n}\left([M_f u_f + M_r u_r]^{n+1} - [M_f u_f + M_r u_r]^n\right) + \nabla \cdot (\vec{V}_f h_f + \vec{H})^{n+1} - Q_f h_f^{n+1} = 0$$

Enthalpy

Internal energy

Advective heat flux

Conductive heat flux

  - Heat flux from Fourier's law: $\vec{H} = -(\lambda_f + \lambda_r)\nabla T$

Governing equations and discretization

- Conservation of energy on semi-discrete, implicit form

$$R_e^{n+1} = \frac{1}{\Delta t^n}([M_f u_f + M_r u_r]^{n+1} - [M_f u_f + M_r u_r]^n) + \nabla \cdot (\vec{V}_f h_f + \vec{H})^{n+1} - Q_f h_f^{n+1} = 0$$

Enthalpy

Internal energy

Advective heat flux

Conductive heat flux

  - Heat flux from Fourier's law: $\vec{H} = -(\lambda_f + \lambda_r)\nabla T$
- Finite-volume + implicit timestepping → stable over wide range of parameters

Newton's method: make system $R(x) = 0$, linearize, neglect higher-order terms

$$x^{k+1} = x^k + \Delta x, \quad -\frac{\partial R}{\partial x}\Delta x = R(x^k)$$

Sequential implicit formulation

1. Form pressure equation as weighted sum of $\mathcal{R}_f$ and $\mathcal{R}_e$

$$\mathcal{R}_p = \omega_f \mathcal{R}_f + \omega_e \mathcal{R}_e, \quad \frac{\partial\big(\omega_f \mathcal{M}_f^{n+1}\big)}{\partial v^i} + \frac{\partial\big(\omega_e [M_f u_f + M_r u_r]^{n+1}\big)}{\partial v^i} = 0, \quad v^i \neq \text{pressure}$$

2. Solve $\mathcal{R}_p = 0$ with fixed temperature and transport variables
   $\rightarrow$ pressure + intercell fluxes
3. Solve $\mathcal{R}_f = 0$ and $\mathcal{R}_e = 0$ with fixed pressure and intercell fluxes
   $\rightarrow$ temperature + transport

Sequential implicit formulation

1. Form pressure equation as weighted sum of $\mathcal{R}_f$ and $\mathcal{R}_e$

$$\mathcal{R}_p = \omega_f \mathcal{R}_f + \omega_e \mathcal{R}_e, \quad \frac{\partial\left(\omega_f \mathcal{M}_f^{n+1}\right)}{\partial v^i} + \frac{\partial\left(\omega_e [M_f u_f + M_r u_r]^{n+1}\right)}{\partial v^i} = 0, \;\; v^i \neq \text{pressure}$$

2. Solve $\mathcal{R}_p = 0$ with fixed temperature and transport variables
   $\rightarrow$ pressure + intercell fluxes
3. Solve $\mathcal{R}_f = 0$ and $\mathcal{R}_e = 0$ with fixed pressure and intercell fluxes
   $\rightarrow$ temperature + transport

Transport formulation: solve for **temperature** T and **total saturation** S_t
$\rightarrow$ allow total saturation to be $\neq 1$, multiply mass and fluxes by total saturation

$$\mathcal{M}_f \rightarrow S_t \mathcal{M}_f u_f, \quad \mu_f \rightarrow \mu_f / S_t, \quad \lambda_\alpha \rightarrow S_t \lambda_\alpha$$

Dynamic coarsening – Coarse grids

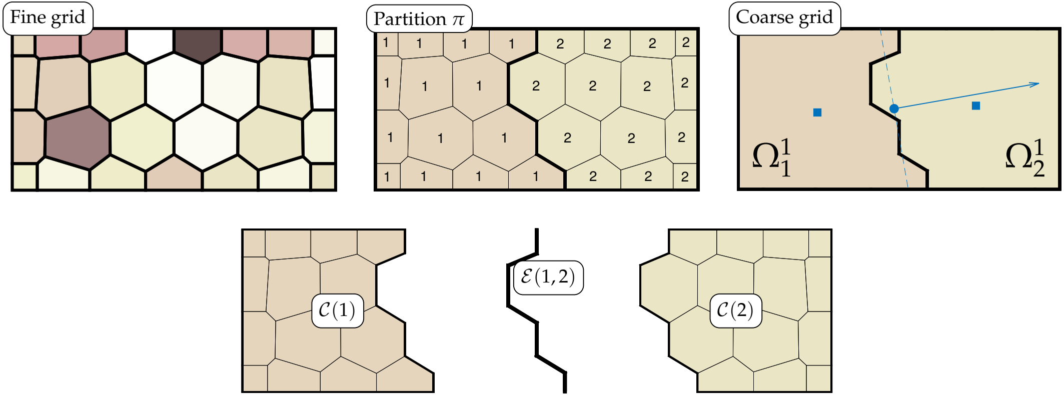

Hauge et al. [2012], Karimi-Fard and Durlofsky [2014], Jones et al. [2020], Klemetsdal and Lie [2020], Klemetsdal et al. [2021]

Dynamic coarsening – Constructing dynamic grids

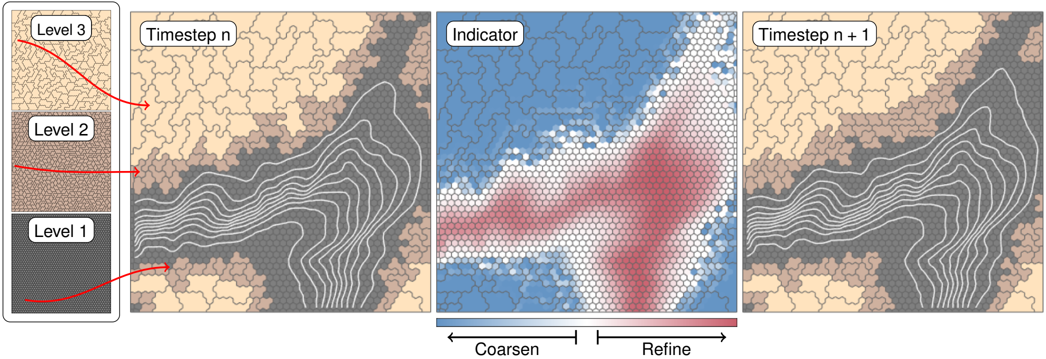

Keep track of which cells to refine/coarsen using coarsening indicator $\mathcal{I}(u) \in \mathbb{R}_+^N$

Coarse block comprising fine-scale cells $\mathcal{C}$

coarsen if $\mathcal{I}_i < \varepsilon_c$ for **all** $i \in \mathcal{C}$, **refine** if $\mathcal{I}_i > \varepsilon_r$ for **any** $i \in \mathcal{C}$

Dynamic coarsening – Mapping quantities

Mapping should be **energy conservative**

$$|\Omega^a|(\mathcal{M}_f^a u_f^a + \mathcal{M}_r^a u_r^a) = \sum_{i \in \mathcal{C}} |\Omega_j|(\mathcal{M}_{f,i} u_{f,i} + \mathcal{M}_{r,i} u_{r,i})$$

1. Pressure, Temperature, and total intercell fluxes

$$\underbrace{p^a = \frac{1}{\phi^a|\Omega^a|} \sum_{i \in \mathcal{C}} \phi_i |\Omega_i| p_i}_{\text{pore-volume-weighted}} \qquad \underbrace{T^a = \frac{1}{\phi^a|\Omega^a|} \sum_{i \in \mathcal{C}} \phi_i |\Omega_i| T_i}_{\text{pore-volume-weighted}} \qquad \underbrace{v^a = \sum_{(m,n) \in \mathcal{E}} v_{mn}}_{\text{sum fine-scale fluxes}}$$

Dynamic coarsening – Mapping quantities

Mapping should be **energy conservative**

$$|\Omega^a|(\mathcal{M}_f^a u_f^a + \mathcal{M}_r^a u_r^a) = \sum_{i \in \mathcal{C}} |\Omega_j|(\mathcal{M}_{f,i} u_{f,i} + \mathcal{M}_{r,i} u_{r,i})$$

1. Pressure, Temperature, and total intercell fluxes

$$\underbrace{p^a = \frac{1}{\phi^a |\Omega^a|} \sum_{i \in \mathcal{C}} \phi_i |\Omega_i| p_i}_{\text{pore-volume-weighted}} \qquad \underbrace{T^a = \frac{1}{\phi^a |\Omega^a|} \sum_{i \in \mathcal{C}} \phi_i |\Omega_i| T_i}_{\text{pore-volume-weighted}} \qquad \underbrace{v^a = \sum_{(m,n) \in \mathcal{E}} v_{mn}}_{\text{sum fine-scale fluxes}}$$

2. Compute energy on adapted grid $\rightarrow |\Omega^a|(\mathcal{M}_f^a u_f^a + \mathcal{M}_r^a u_r^a)$

Dynamic coarsening – Mapping quantities

Mapping should be **energy conservative**

$$|\Omega^a|(\mathcal{M}_f^a u_f^a + \mathcal{M}_r^a u_r^a) = \sum_{i \in \mathcal{C}} |\Omega_j|(\mathcal{M}_{f,i} u_{f,i} + \mathcal{M}_{r,i} u_{r,i})$$

1. Pressure, Temperature, and total intercell fluxes

$$\underbrace{p^a = \frac{1}{\phi^a|\Omega^a|} \sum_{i \in \mathcal{C}} \phi_i |\Omega_i| p_i}_{\text{pore-volume-weighted}} \qquad \underbrace{T^a = \frac{1}{\phi^a|\Omega^a|} \sum_{i \in \mathcal{C}} \phi_i |\Omega_i| T_i}_{\text{pore-volume-weighted}} \qquad \underbrace{v^a = \sum_{(m,n) \in \mathcal{E}} v_{mn}}_{\text{sum fine-scale fluxes}}$$

2. Compute energy on adapted grid $\rightarrow |\Omega^a|(\mathcal{M}_f^a u_f^a + \mathcal{M}_r^a u_r^a)$
3. Set total saturation equal to **energy discrepancy**

$$S_t = \frac{\sum_{i \in \mathcal{C}} |\Omega_j|(\mathcal{M}_{f,i} u_{f,i} + \mathcal{M}_{r,i} u_{r,i})}{|\Omega^a|(\mathcal{M}_f^a u_f^a + \mathcal{M}_r^a u_r^a)} = \frac{\text{accumulated energy from fine grid}}{\text{energy on adapted grid}}$$

Example: SPE10 Model 2

- Heat storage in two different layers of SPE10 Model 2
- Three one-year cycles of storage in center well with pressure support in corner wells
  1. **Load phase:** 3 months of injection at 80 °C, bhp = 70 bar
  2. **Rest phase:** 3 months with no driving forces
  3. **Unload phase:** 3 months of extraction, bhp = 1500 bar
  4. **Rest phase:** 3 months with no driving forces
- Three coarsening approaches
  1. Static based on incompressible time-of-flight
  2. Dynamic with residual-based indicator
  3. Dynamic with temperature indicator

Example: SPE10 Model 2 – Tarbert Formation (layer 10)

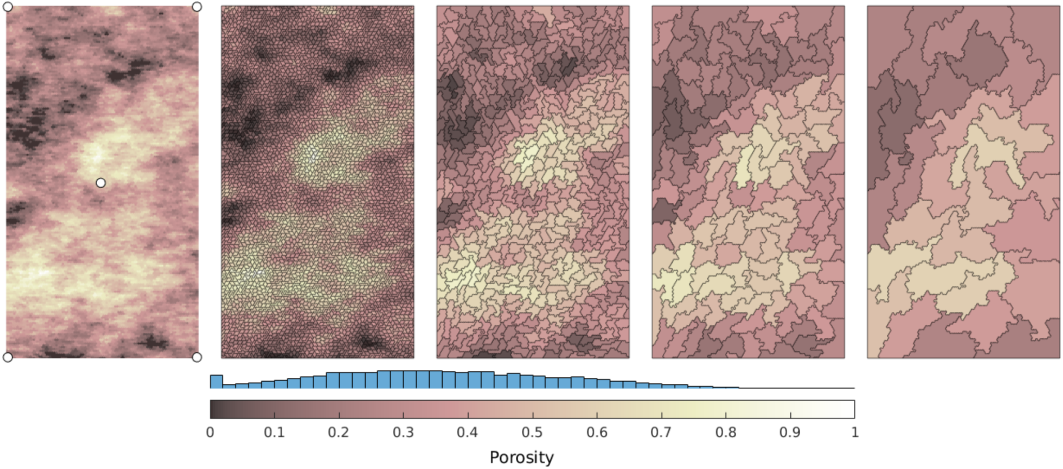

Example: SPE10 Model 2 – Tarbert Formation (layer 10)

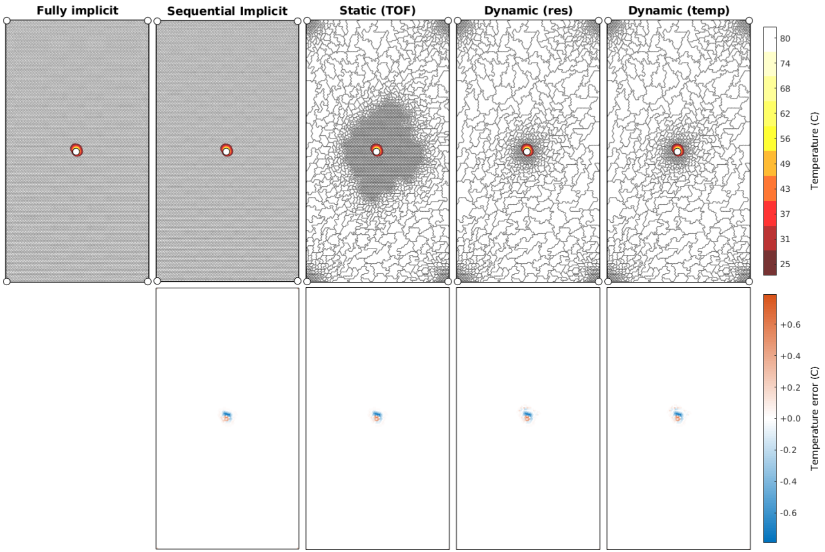

Example: SPE10 Model 2 – Tarbert Formation (layer 10)

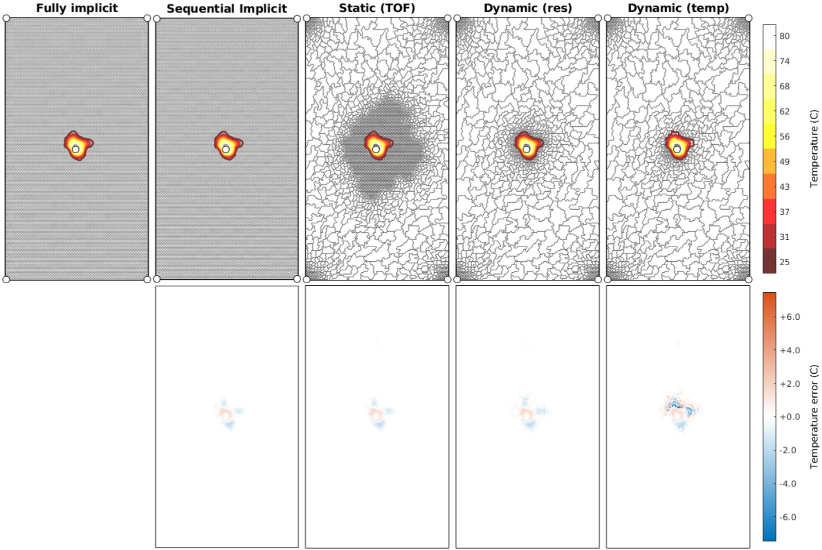

Example: SPE10 Model 2 – Tarbert Formation (layer 10)

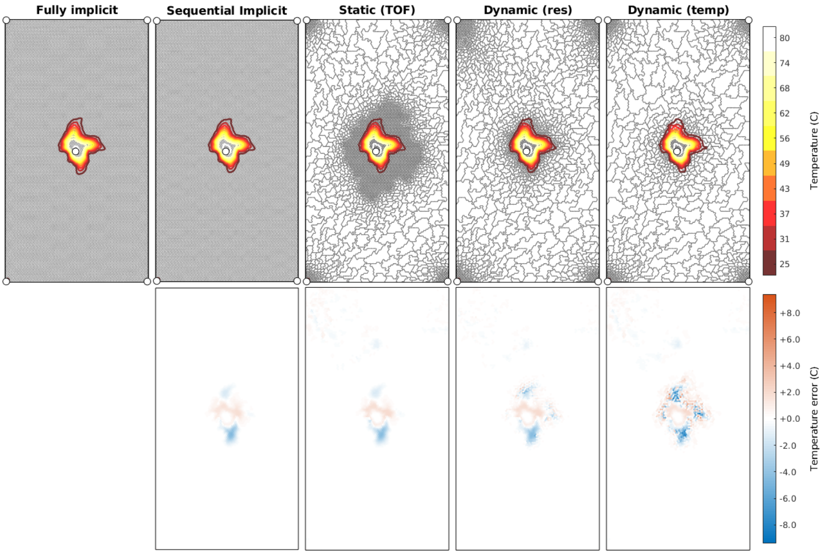

Example: SPE10 Model 2 – Tarbert Formation (layer 10)

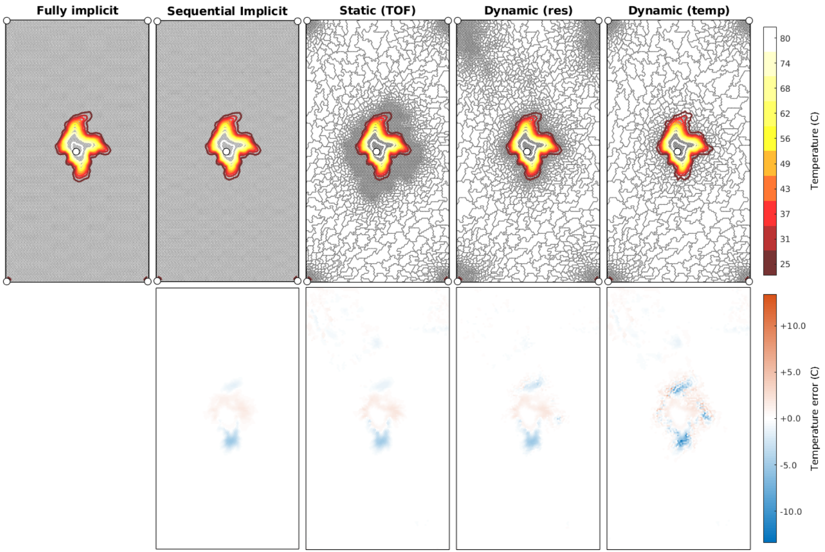

Example: SPE10 Model 2 – Tarbert Formation (layer 10)

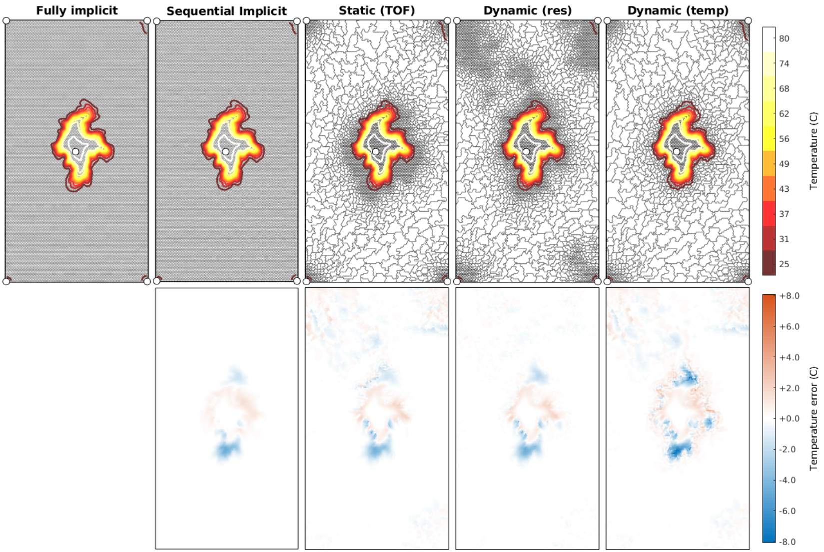

Example: SPE10 Model 2 – Tarbert Formation (layer 10)

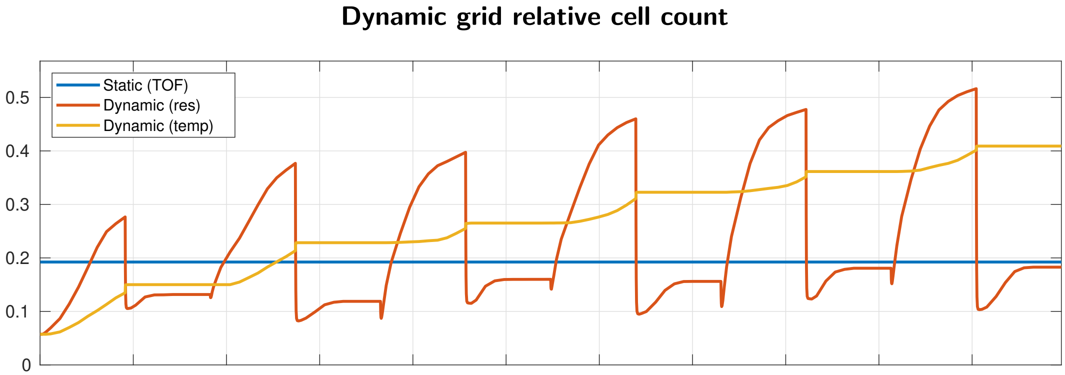

Example: SPE10 Model 2 – Tarbert Formation (layer 10)

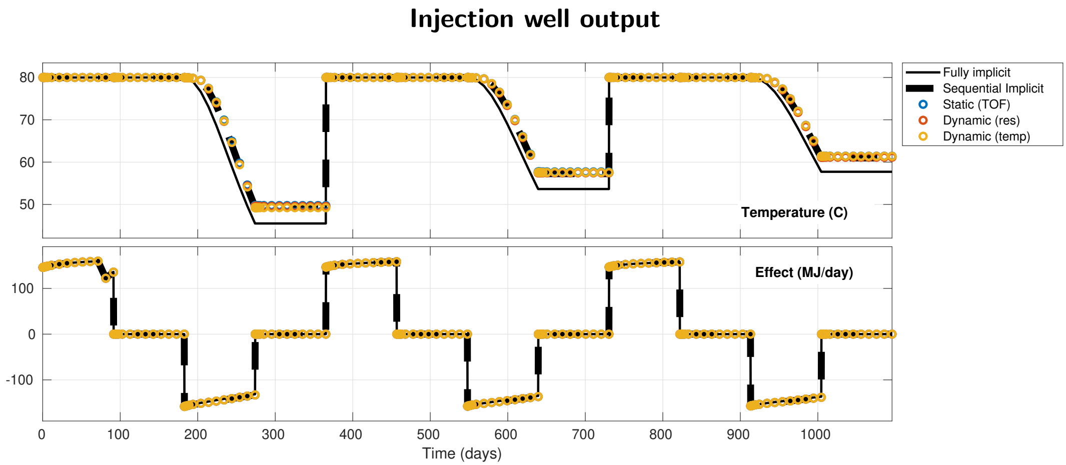

Example: SPE10 Model 2 – Upper Ness Formation (layer 85)

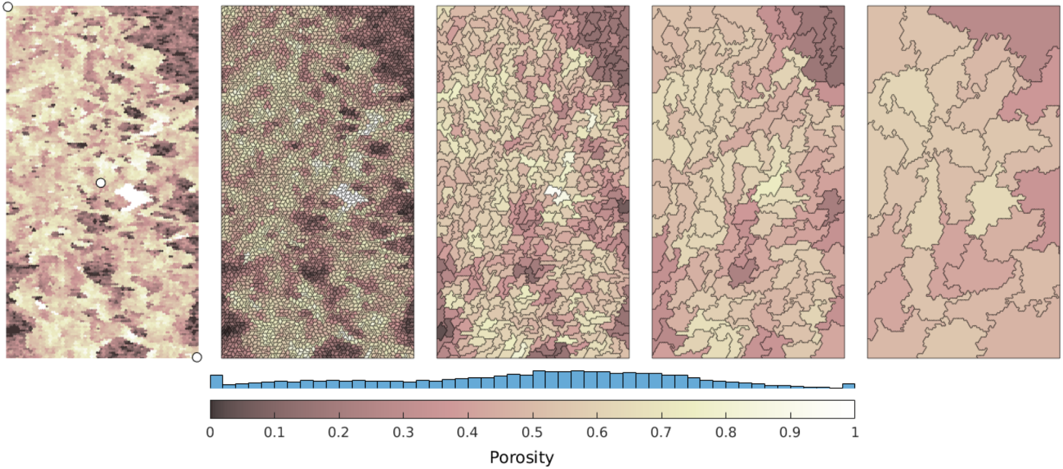

Example: SPE10 Model 2 – Upper Ness Formation (layer 85)

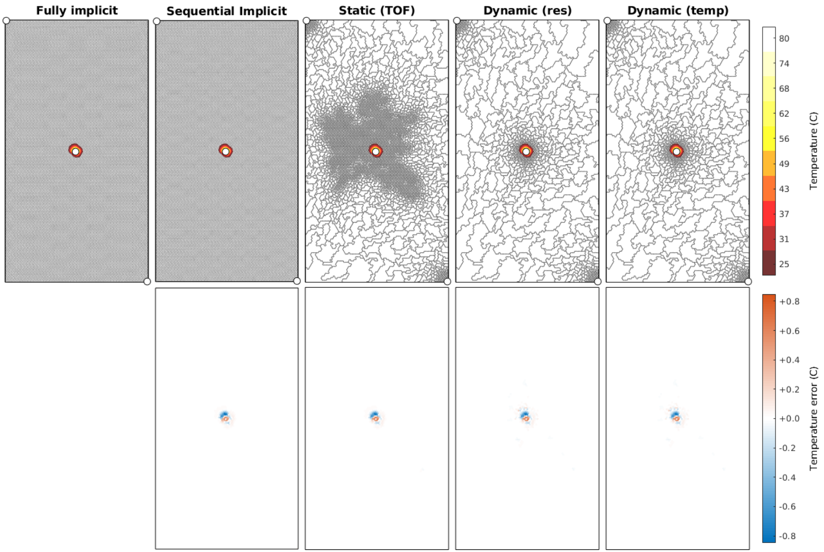

Example: SPE10 Model 2 – Upper Ness Formation (layer 85)

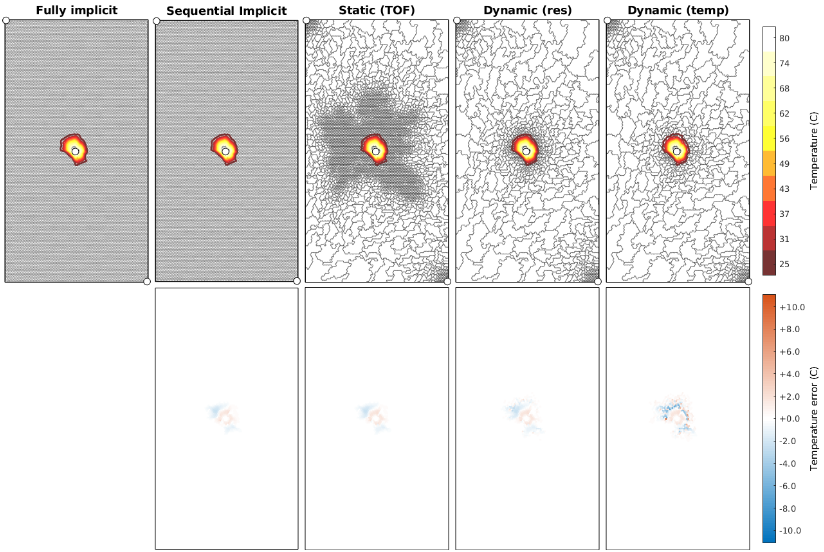

Example: SPE10 Model 2 – Upper Ness Formation (layer 85)

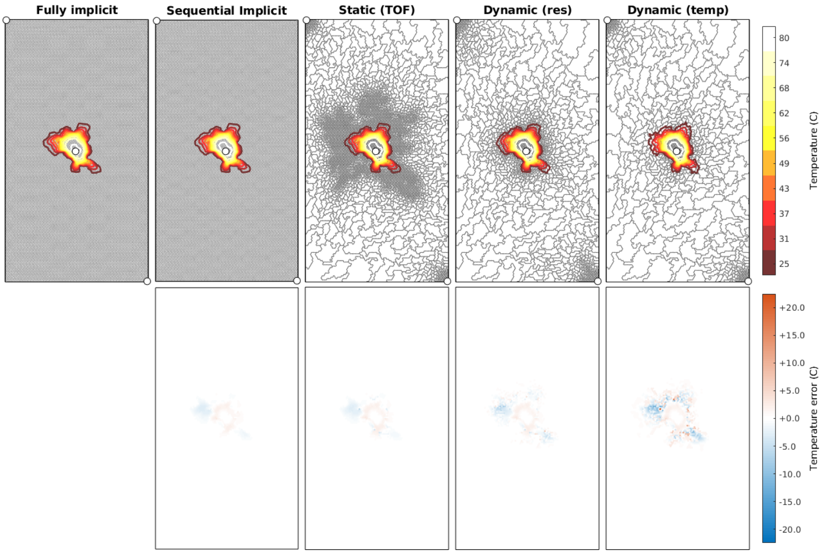

Example: SPE10 Model 2 – Upper Ness Formation (layer 85)

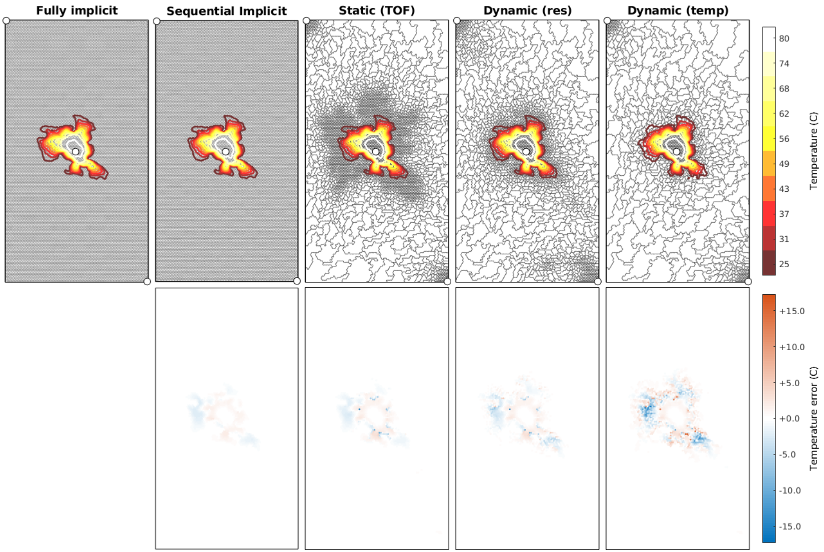

Example: SPE10 Model 2 – Upper Ness Formation (layer 85)

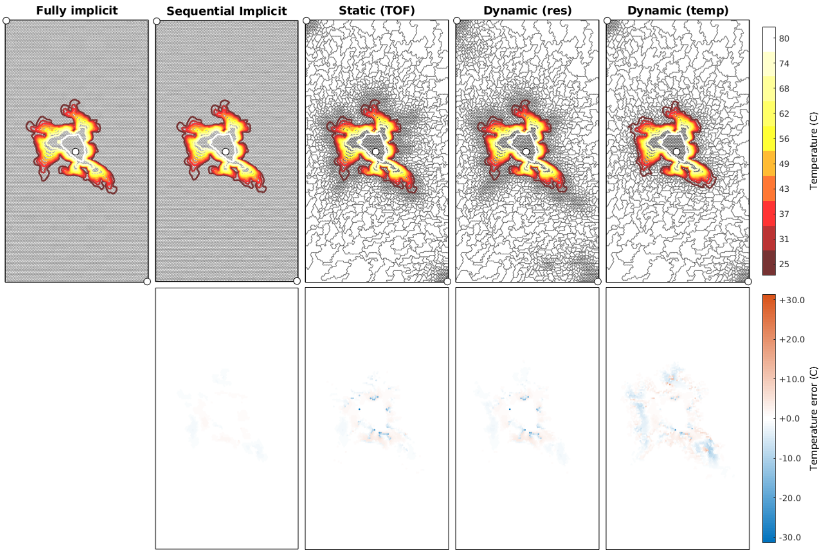

Example: SPE10 Model 2 – Upper Ness Formation (layer 85)

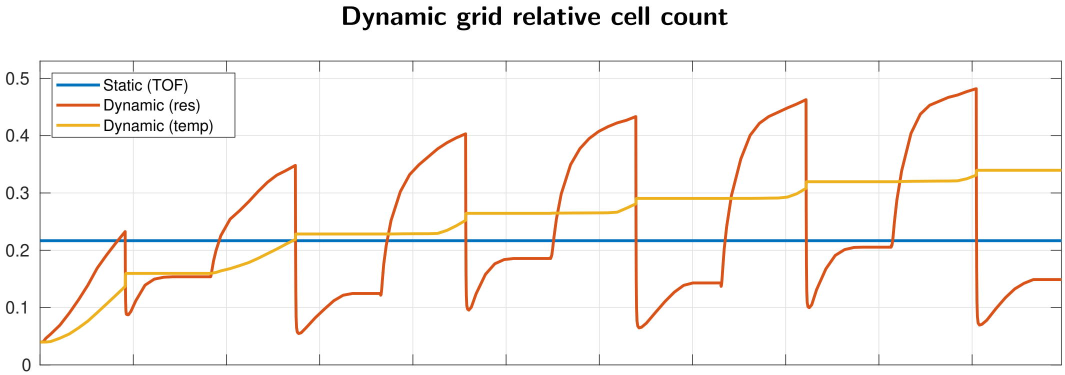

Example: SPE10 Model 2 – Upper Ness Formation (layer 85)

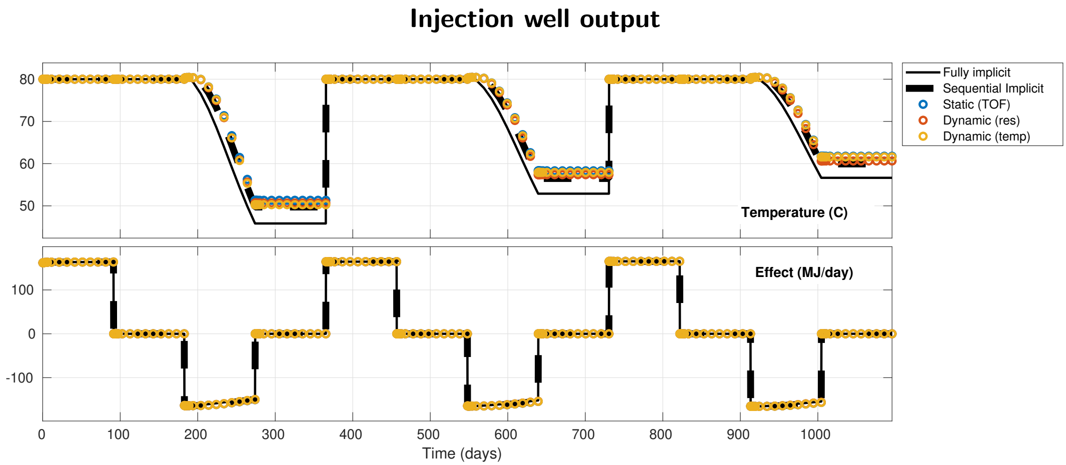

Example: SPE10 Model 2

- Very close match with fine-scale results for all indicators and coarsening strategies
  - Between 49% and 96% reduction in # transport problem dofs
- Point-wise large temperature differences
- Energy discrepancy correction ensures conservation of energy between scales

Example: Real(istic) Model

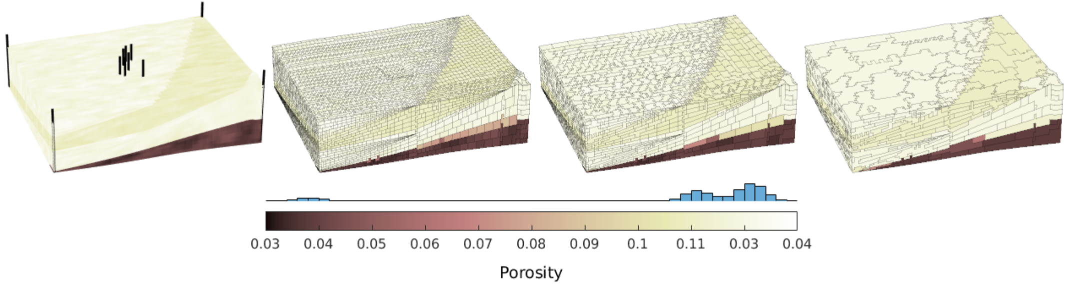

- Model of real geothermal storage site, provided by Ruden AS
- Group of wells in the center inject at 73 °C over period of four months
- Corner wells provide pressure support
- Dynamic coarsening with residual-based indicator

Reservoir temperature

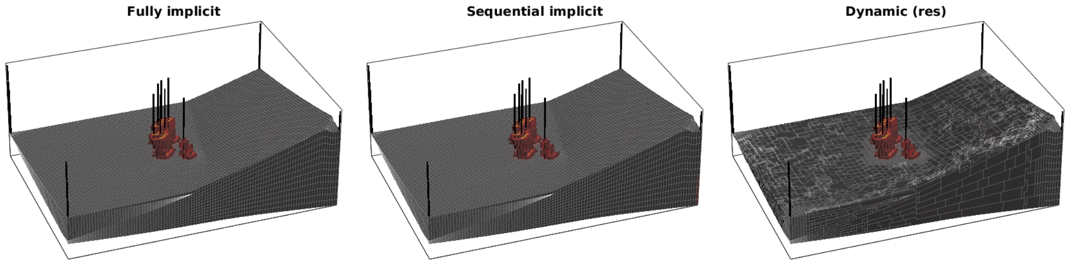

Example: Real(istic) Model

Reservoir temperature

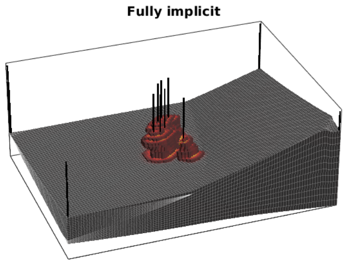

Reservoir temperature

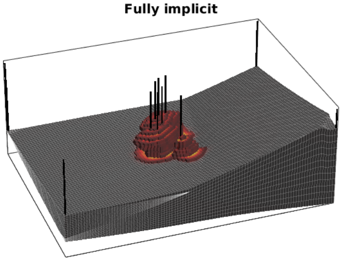

Example: Real(istic) Model

Reservoir temperature

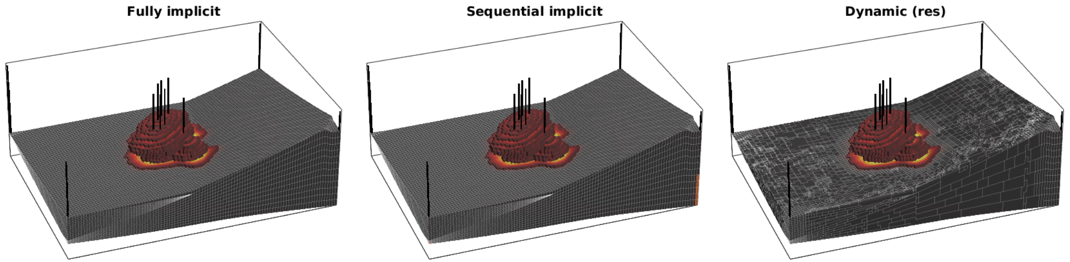

Example: Real(istic) Model

Relative L_2 error and dynamic grid relative cell count

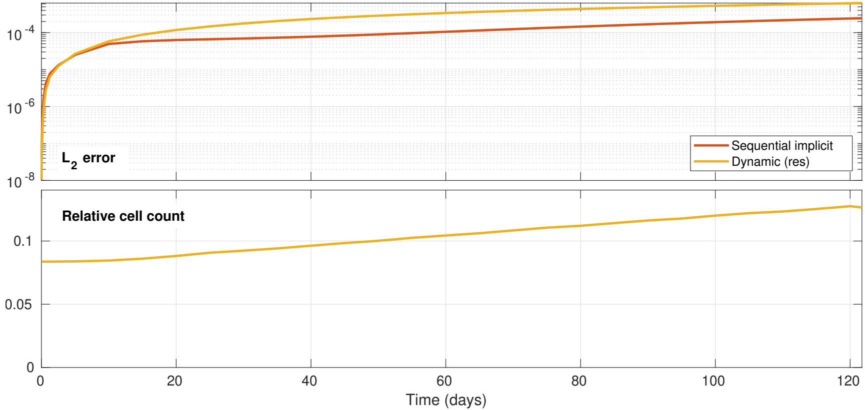

Example: Real(istic) Model

Relative L_2 error and dynamic grid relative cell count

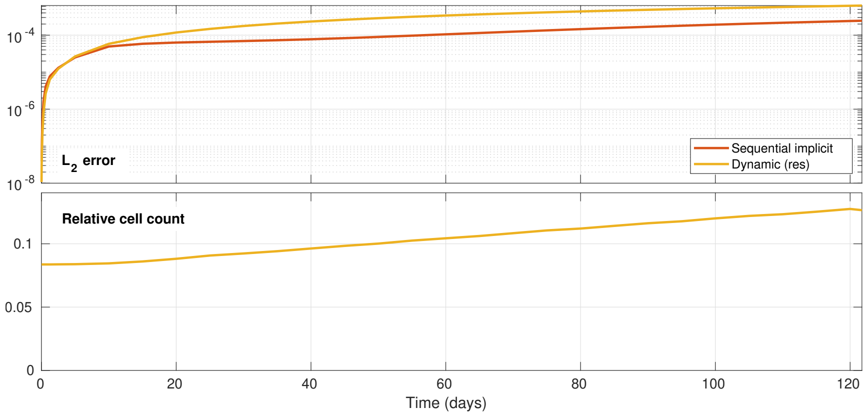

Less than 10^{-3} maximum relative L_2 error with at least **87% reduction** in # transport problem dofs

Concluding Remarks

Conclusions

- Highly flexible **dynamic coarsening** method for geothermal simulations in MRST
  - Sequential splitting of flow and transport/energy
  - Applicable to unstructured, polytopal grids
  - Energy discrepancy correction ensures **conservation of energy**
  - Capable of simulating low- to moderate enthalpy geothermal systems
- Method demonstrated on two examples
  - **Significant reduction** in # dofs in the transport subproblem
  - Very good match with fine-scale solution

Concluding Remarks

Conclusions

- Highly flexible **dynamic coarsening** method for geothermal simulations in MRST
  - Sequential splitting of flow and transport/energy
  - Applicable to unstructured, polytopal grids
  - Energy discrepancy correction ensures **conservation of energy**
  - Capable of simulating low- to moderate enthalpy geothermal systems
- Method demonstrated on two examples
  - **Significant reduction** in # dofs in the transport subproblem
  - Very good match with fine-scale solution

Further work

- Optimize implementation and investigate actual CPU speedup
- Test method for high-enthalpy systems (phase changes)
- Solve each subproblem at its appropriate timescale
  - Multiple transport steps for each pressure step

Acknowledgements

Thanks to Marine Collignon (Uni Geneva), Olav Møyner and Knut-Andreas Lie (SINTEF Digital) for valuable support and discussions

Thanks to Ruden AS for allowing use of the field model in this work

References

O. Andersson. Aquifer thermal energy storage. In *Thermal Energy Storage for Sustainable Energy Consumption: Fundamentals, Case Studies and Design*, chapter 8, pages 155–176. Springer, 2007. doi: 10.1007/978-1-4020-5290-3.

W. Glassley. *Geothermal Energy: Renewable Energy and the Environment*. CRC Press, 2010. doi: 10.1201/b17521.

V. L. Hauge, K.-A. Lie, and J. R. Natvig. Flow-based coarsening for multiscale simulation of transport in porous media. *Comput. Geosci.*, 16(2): 391–408, 2012. ISSN 14200597. doi: 10.1007/s10596-011-9230-x. URL http://link.springer.com/10.1007/s10596-011-9230-x.

P. Jenny, S. H. Lee, and H. A. Tchelepi. Adaptive fully implicit multi-scale finite-volume method for multi-phase flow and transport in heterogeneous porous media. *Journal of Computational Physics*, 217(2):627–641, 2006. doi: 10.1016/j.jcp.2006.01.028.

E. Jones, S. D. Hoop, and D. Voskov. Adaptive Mesh Refinement for Thermal-Reactive Flow and Transport on Unstructured Grids. In *ECMOR XVII - 17th Eur. Conf. Math. Oil Recover.*, number September 2020, 2020.

M. Karimi-Fard and L. Durlofsky. Unstructured adaptive mesh refinement for flow in heterogeneous porous media. volume 2014, pages 1–9. European Association of Geoscientists & Engineers, 2014. doi: https://doi.org/10.3997/2214-4609.20141856. URL https://www.earthdoc.org/content/papers/10.3997/2214-4609.20141856.

Ø. S. Klemetsdal and K.-A. Lie. Dynamic coarsening and local reordered nonlinear solvers for simulating transport in porous media. *SPE J.*, (January):1–20, 2020. doi: 10.2118/201089-PA.

Ø. S. Klemetsdal, O. Møyner, H. M. Nilsen, A. Moncorgé, and K.-A. Lie. High-resolution compositional reservoir simulation with dynamic coarsening and local timestepping for unstructured grids, 2021.

K. S. Lee. A review on concepts, applications, and models of aquifer thermal energy storage systems. *Energies*, 3(6):1320–1334, 2010. doi: 10.3390/en3061320.

K.-A. Lie, O. Møyner, J. R. Natvig, A. Kozlova, K. Bratvedt, S. Watanabe, and Z. Li. Successful application of multiscale methods in a real reservoir simulator environment. *Computational Geosciences*, 21(5-6):981–998, 2017. doi: 10.1007/s10596-017-9627-2.

O. Møyner and K.-A. Lie. A multiscale restriction-smoothed basis method for high contrast porous media represented on unstructured grids. *Journal of Computational Physics*, 304:46–71, 2016. doi: 10.1016/j.jcp.2015.10.010.

M. J. O'Sullivan, K. Pruess, and M. J. Lippmann. Geothermal reservoir simulation: the state-of-practice and emerging trends. In *Proceedings of the World Geothermal Congress*, 2000.

I. Stober and K. Bucher. *Geothermal Energy: From theoritical Models to Exploration and development*. Springer, 2013.